Dynamic Study and Structural Optimization of the Connecting Rod from a Thermal Combustion Engine

IONUT GEONEA[1], CRISTIAN COPILUSI[1], LAURENTIU RACILA[1],
DANIELA ANTONOVA SHEHOVA[2], SLAVI YASENOV LYUBOMIROV [2],
EMIL GEORGIEV VELEV[3]
[1] University of Craiova, Faculty of Mechanics, Department of Applied Mechanics and Civil Construction, Craiova, Romania
[2] Paisii Hilendarski University of Plovdiv, Faculty of Physics and Technology, Department of Power Engineering and Communications, Plovdiv, Bulgaria
[3] Paisii Hilendarski University of Plovdiv, Faculty of Physics and Technology, Department of Mechanical Engineering and Transport, Plovdiv, Bulgaria
ionut.geonea@edu.ucv.ro

Abstract

In this paper, we present research on the structural optimization of a rod in a 1-cylinder in-line thermal engine structure. To perform this optimization, we will use the finite element analysis program, ANSYS. We will parametrically model the connecting rod using ANSYS Design Modeler. Some geometrical dimensions, such as the radii of the connection, and the relief channels, we will consider as structural optimization parameters. The objective function of this optimization is to reduce stress concentrators, with the aim of increasing fatigue strength, but also to reduce connecting rod mass. We will present the results obtained, in the form of 3D graphs. We will present the optimal solution for the geometrical shape of the connecting rod. The study demonstrates the effectiveness of structural optimization programs to achieve optimal part design shapes effect.

Keywords: Structural Optimization, Engine Dynamic model, Multibody Simulation.

1. Introduction

Finite element analysis of the connecting rod of an internal combustion engine is a research topic for many authors [1, 2, 3]. In addition to structural analysis, in the literature, we find studies that address the analysis of structural integrity in terms of resistance to fatigue [4, 5]. The most widely used software for checking structural integrity with finite elements is ANSYS [1]. There is research [6], which shows that aluminium alloys are also used to manufacture the connecting rod, in order to reduce the mass. In order to validate the structural integrity of any type of designed part, the first step is that of the structural analysis with FEM. The ANSYS program allows us to perform an analysis of the strength of the connecting rod made of metal powders, taking into account the material and its mechanical properties. In addition to validating the construction of the connecting rod, this analysis allows us to validate the material

based on titanium alloy, as a solution for the manufacture of a heat engine connecting rod, namely: high mechanical strength combined with a low specific mass (material density is 3.63grams / centimeter^3).

2. Dynamic analysis of the thermal combustion engine rod considered as a deformable solid

2.1. Theoretical background of dynamic modal analysis with MSC Adams software

In this paragraph, we will present some theoretical aspects of dynamic modal analysis with MSC ADAMS software. This is necessary because, in the dynamic simulation in ADAMS, it is important to consider the connecting rod as a deformable solid. Modal superposition is valorised in two key areas:

• Flexible kinematics of markers;

• Equations of motion of flexible bodies.

Marker kinematics refers to marker position, orientation, speed, and acceleration. ADAMS uses marker kinematics in three essential areas:

• Markers' position and orientation must be known to satisfy constraints such as those imposed in the JOINT and JPRIM elements.

• To project the point forces applied to the generalized coordinates of the flexible body markers.

• Marker measures (for example DX, WZ, PHI, ACCX, and so on), require information about the position, orientation, velocity, and acceleration of the markers.

The instantaneous position of a marker that is attached to node *P*, on a flexible body, *B*, is the sum of three vectors (Figure 1).

$$r_p = \vec{x} + \vec{s}_p + \vec{u}_p \qquad (1)$$

where: $\vec{x}$ is the position vector from the origin of the fixed reference system, to the origin of the local reference system, *B* of the flexible body; $\overrightarrow{Sp}$ - the position vector of the undeformed location of point *P*, relative to the local reference system attached to body *B*; $\overrightarrow{Up}$ - is the translation of the deformation vector of point P, the position vector from the location of the undeformed point to the deformed location.

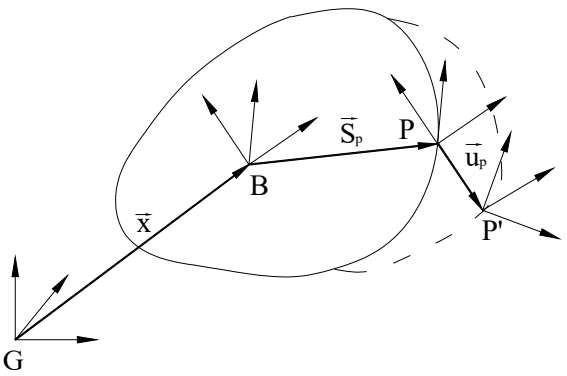

Figure 1. The position vector of the deformation point *P′* of a flexible body relative to a reference system attached to the body *B* and the fixed base *G*

If we rewrite equation (1) in a matrix form, expressed in relation to the basic coordinate system:

$$r_p = x + {}^{G}A^{B}\left(s_p + u_p\right) \tag{2}$$

where: x is the position vector, from the origin of the fixed system to the origin of the local reference system attached to the flexible body B, expressed in the fixed (basic) coordinate system. The elements of the vector $\vec{x}$, namely x, y and z, are the generalized coordinates of the flexible body; Sp is the position vector from the local reference system B to point P, expressed in the body's local coordinate system, which is constant; ${}^{G}A^{B}$ - is the transformation matrix from the local reference system in B to the base system. This matrix is known as being formed with the principal cosines of the local reference system relative to the fixed one. Orientation is calculated using Euler's angles, Ψ, θ, and Φ. Euler's angles are the generalized coordinates of the flexible body; u_p is the translational strain vector of point P, also expressed in the local coordinate system attached to the body. The strain vector is a superposition of shape functions:

$$u_p = \Phi_p q \tag{3}$$

where: Φp, is the part of the matrix of shape functions that corresponds to the translational degrees of freedom for the node P.

Matrix size Φp is $3xM$, where M is the number of shape functions. Coordinates of shape functions q_i, ($i=1...M$) are the generalized coordinates of the flexible body.

Thus, the generalized coordinates of the flexible body are:

$$\xi = \begin{Bmatrix} x \\ y \\ z \\ \psi \\ \theta \\ \varphi \\ q_{i,\,(i=1\ldots M)} \end{Bmatrix} = \begin{Bmatrix} x \\ \psi \\ q \end{Bmatrix} \tag{4}$$

The equations governing a flexible body are derived from Lagrange's equations:

$$\frac{d}{dt}\left(\frac{\partial L}{\partial \dot{\xi}}\right) - \frac{\partial L}{\partial \xi} + \frac{\partial F}{\partial \dot{\xi}} + \left[\frac{\partial \Psi}{\partial \xi}\right]^{T} \lambda - Q = 0, \Psi = 0 \tag{5}$$

where: L is the Lagrangian, defined: $L=T-V$, T, and V represent the kinetic energy, respectively potential energy; F is the energy dissipation function defined; Ψ are the constraint equations; λ are the Lagrange multipliers for the constraints; ξ is the defined generalized coordinates; Q are the applied generalized forces (the applied forces projected on ξ).

2.2. Dynamic modal analysis with MSC Adams for an internal combustion engine

To create the dynamic model in ADAMS we went through the following steps:

1. We have defined the materials corresponding to the kinematic elements, as well as the kinematic couples related to the model.
2. We have specified the variation law of the pressure inside the combustion chamber, corresponding to an engine cycle.

The variation law of the pressure inside the combustion chamber, corresponding to a complete engine cycle, i.e. two revolutions of the crankshaft [7], is shown in Figure 2.

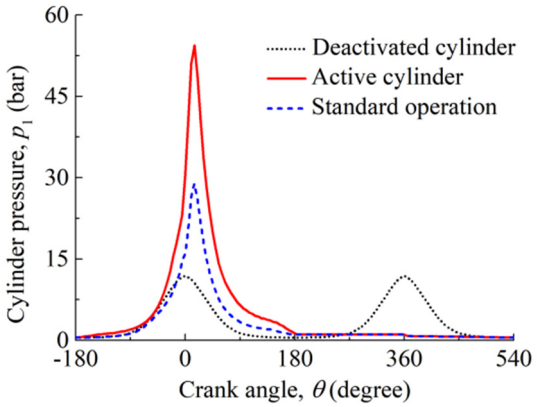

Figure 2. Pressure variation law in the combustion chamber, during the combustion process

The diagram for pressure (MPa) is reported in Figure 2. Based on the spline function we will define the force on the piston head. Obviously, the pressure value must be multiplied by the surface area of the piston (Area of a circle). The force is defined, with function Builder, based on the spline built with experimental data, and the Akima Fitting Method. Press the Assist button, and the Akima Fitting Method window appears. The first independent variable is time, then the constructed spline function will be selected.

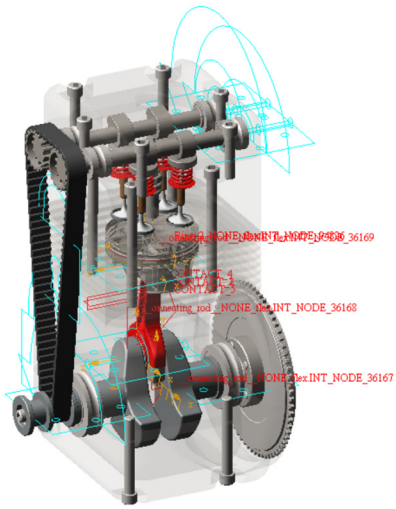

Figure 3. The thermal combustion engine virtual model imported in MSC Adams for virtual dynamic simulations

In Figure 4 it is shown the connecting rod of the mechanism is defined as a deformable solid one.

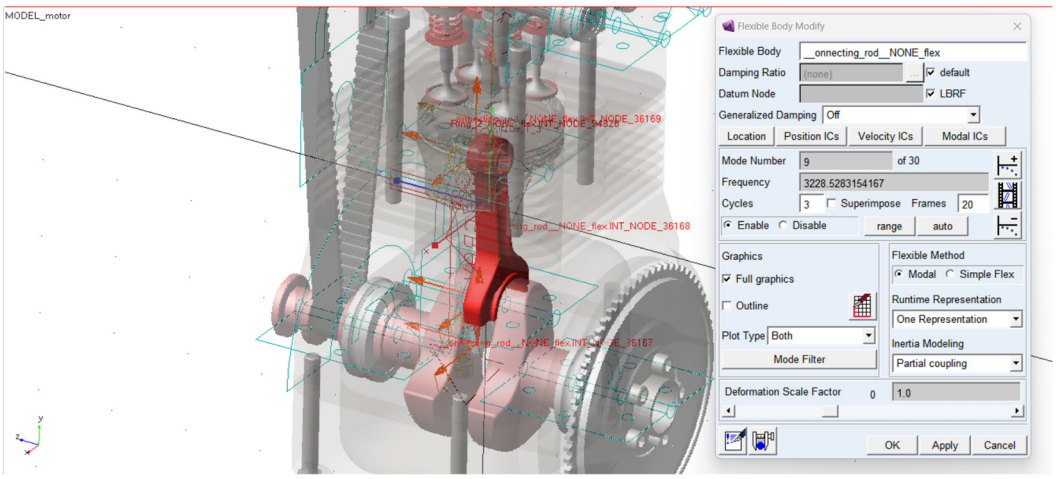

Figure 4. Defining the connecting rod of the thermal engine as a deformable solid one, through the mesh option in the finite elements simulations

The results presented below are graphs that show the variation over time of the translational deformation, the speed, and the deformation acceleration of the marker attached to the centre of connecting rod mass.

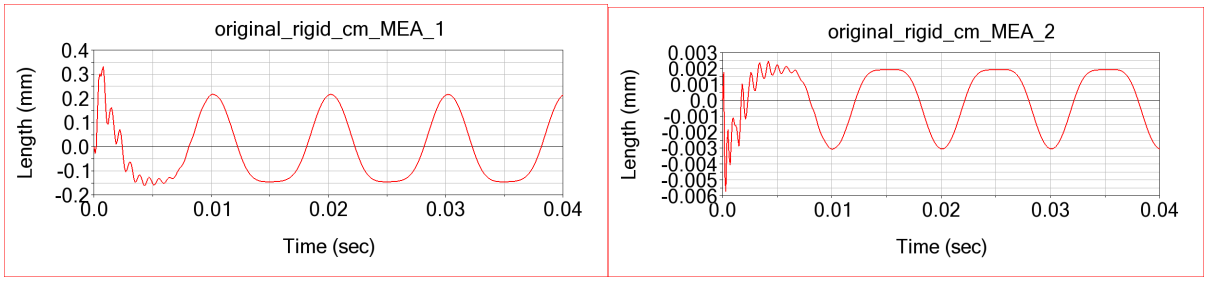

Figure 5. Deformations variation laws for the marker attached to the centre of mass of the connecting rod along the X and Y axes, relative to the global axis system

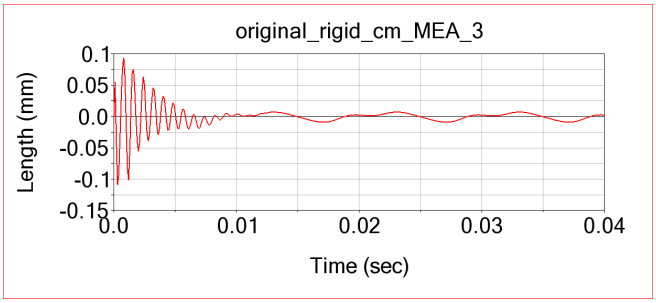

Figure 6. Deformations variation laws for the marker attached to the centre of mass of the connecting rod along the Z axis, relative to the global axis system

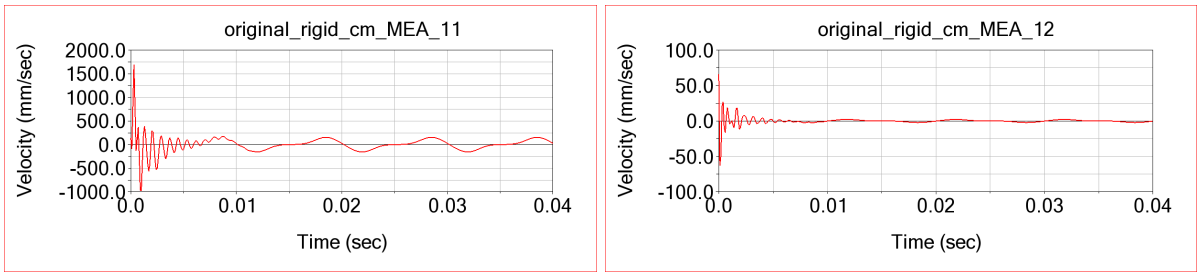

Figure 7. Velocity variation laws for the marker attached to the centre of mass of the connecting rod along the X and Y axes, relative to the global axis system

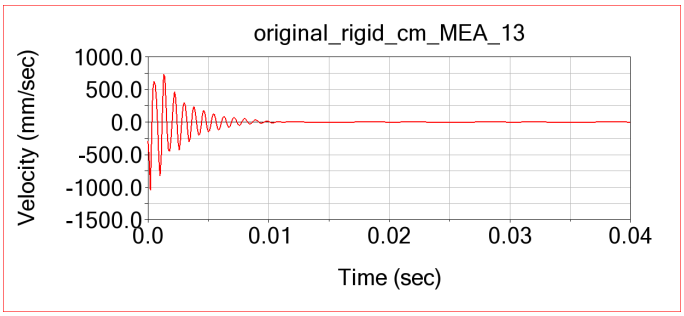

Figure 8. Velocity variation laws for the marker attached to the centre of mass of the connecting rod along the Z axis, relative to the global

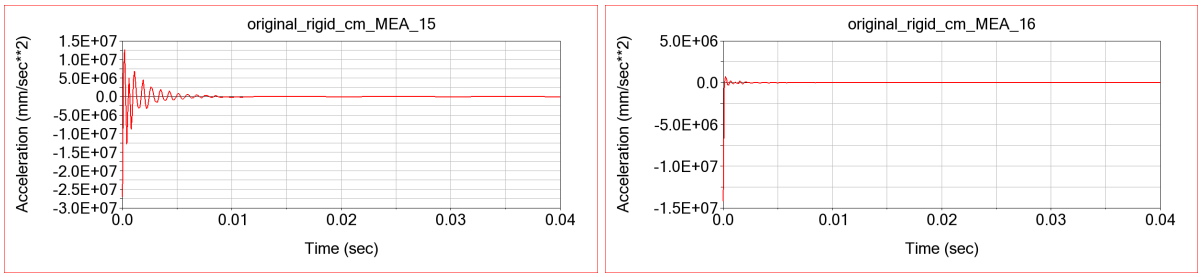

Figure 9. Acceleration variation laws for the marker attached to the centre of mass of the connecting rod along the X and Y axes, relative to the global

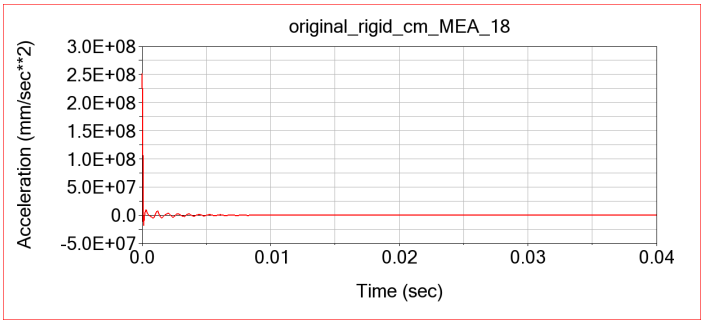

Figure 10. Acceleration variation laws for the marker attached to the centre of mass of the connecting rod along the Z axis, relative to the global

These values obtained for the parameters presented above fall within the normal operating limits.

3. Connecting rod structural optimization with the finite element method

In this paragraph, we propose to carry out the structural optimization of the connecting rod of a heat engine. For this study, we will use the finite element analysis program ANSYS, and we will use the ANSYS Workbench module.

The block diagram of the connecting rod structural optimization process is shown in Figure 11.

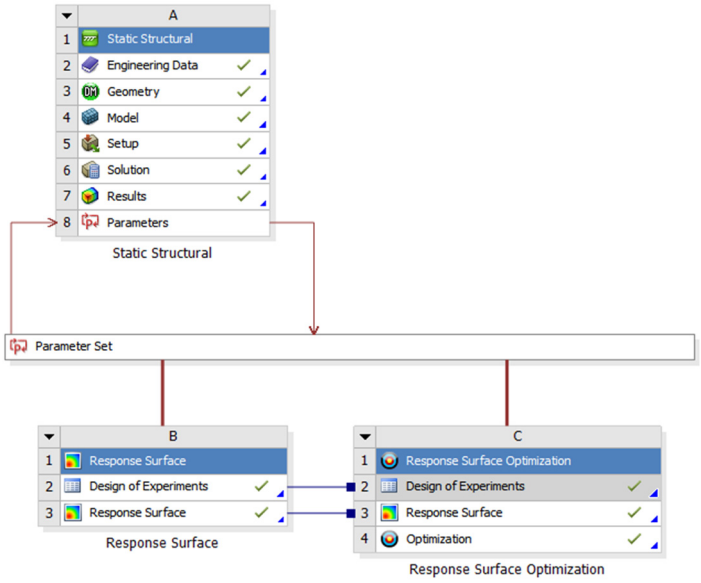

Figure 11. Block diagram of the connecting rod optimization process

The successive steps taken, according to the block diagram, are detailed below. It is observed that in the first stage, we have to choose the type of finite element analysis desired, which is structural static. The next stage allows us to choose the material from the "Engineering data" database, or to define the characteristic properties of a material.

A very important stage is the construction of the geometry of the part, which must be defined parametrically so that it can be modified in order to obtain the optimal geometry. The optimization with finite elements has as important objectives: Reducing the mass of the piece; Reducing stress concentrators in the part.

The part geometry can be made with two tools available in ANSYS Workbench, namely: Ansys Space Claim and Ansys Design Modeler.

In this application, we will choose to create the geometry using Ansys Design Modeler. For this, we will use an execution drawing from a connecting rod that exists on a thermal engine.

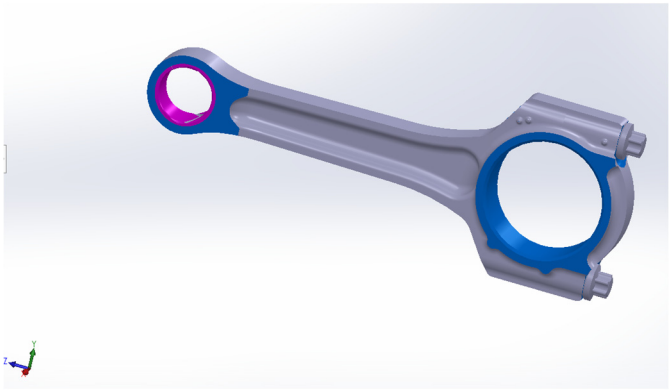

Figure 12. The existing connecting rod on a thermal engine

Through the geometric construction tools in ANSYS Design Modeler, we will make the first sketch, as shown in Figure 13.

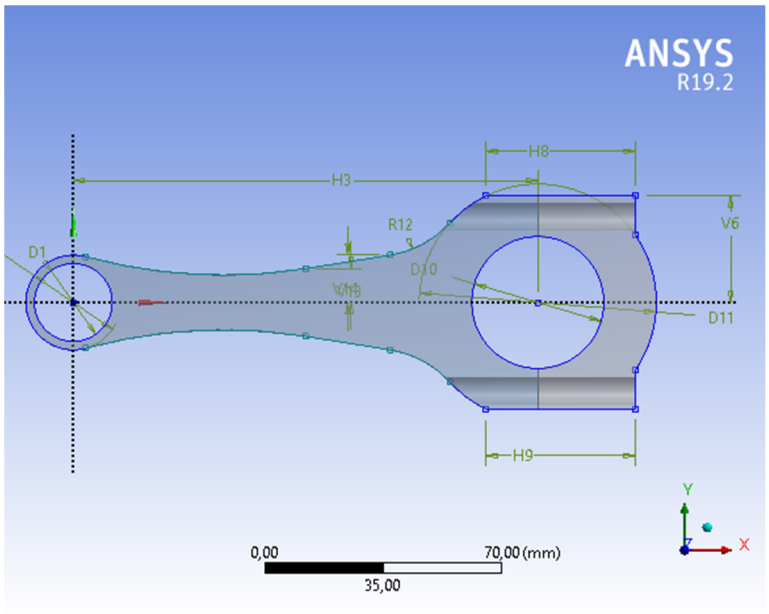

Figure 13. Making the first sketch, based on which the profile of the connecting rod will be made by extrusion

The values of these parameters, which are indicated in Figure 13, have the numerical values specified in Figure 14.

Details View

Show Constraints?	No
Dimensions: 11	
D1	23 mm
D10	39 mm
D11	70 mm
D D4	28 mm
H3	137 mm
H8	44 mm
H9	44 mm
D R12	30 mm
V13	10 mm
V14	14 mm
V6	31,5 mm

Figure 14. Design parameters initial values

The extrusion of this first sketch, indicated in Figure 3 will be made along the length of 15 millimetres, as shown in Figure 15, where we see the discretized connecting rod in finite elements.

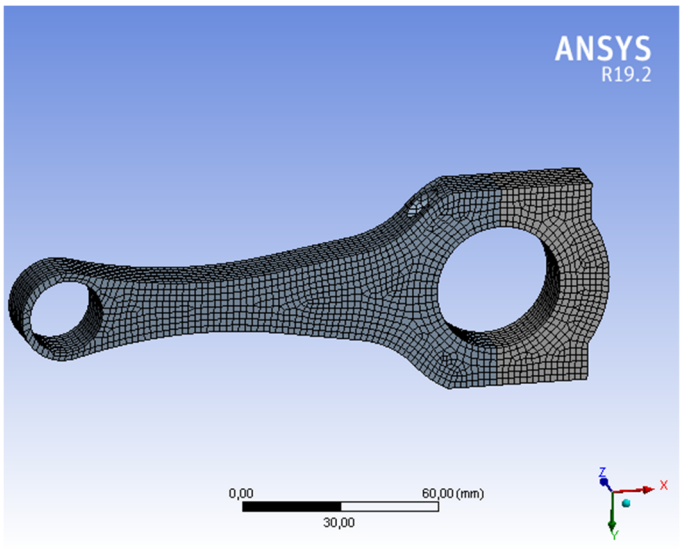

Figure 15. Connecting rod finite element meshing

As for the equivalent stresses obtained, their distribution is shown in Figure 16. The maximum value is 39.095 MPa and it can be seen that the piece does not present stress concentrators.

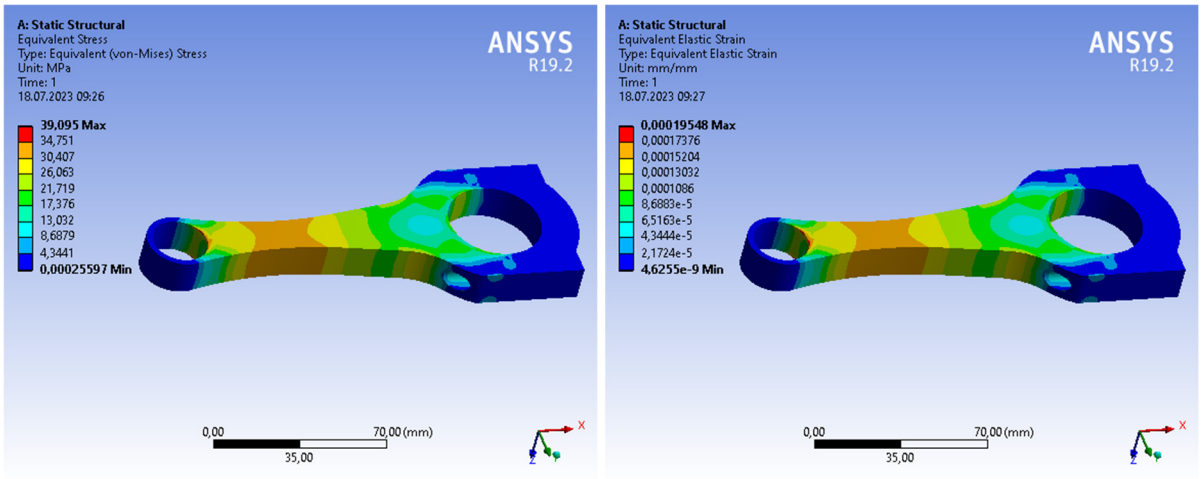

Figure 16. Von Misses equivalent stress distribution for the analysed connecting rod

The steps of the structural optimization of the connecting rod are the following: Design parameters are defined, namely: Diameter D4 and radius R12 (see Figure 13); Definition of design parameters; Definition of the output parameters, i.e. the mass of the connecting rod and the maximum value of the equivalent stress; Running "Design of Experiments".

For each input parameter, the variation limits are defined, i.e. the minimum and maximum possible value, as shown in Figure 17.

Properties of Outline A5: P1 - XYPlane.D4

	A	B
1	Property	Value
2	General	
3	Units	mm
4	Type	Design Variable
5	Classification	Continuous
6	Values	
7	Lower Bound	25,2
8	Upper Bound	30,8
9	Allowed Values	Manufacturable Values
10	Number Of Levels	2

Properties of Outline A6: P2 - XYPlane.R12

	A	B
1	Property	Value
2	General	
3	Units	mm
4	Type	Design Variable
5	Classification	Continuous
6	Values	
7	Lower Bound	27
8	Upper Bound	33
9	Allowed Values	Manufacturable Values
10	Number Of Levels	2

Figure 17. Design variables limit definition

With this data, a number of 10 possible design variants are calculated as shown in Figure 18. For each of these design variants, the program calculates the values of the output parameters, which are shown in columns D, E and F from Figure 18. The response surface will be evaluated as it can be remarked in Figure 19.

Table of Outline A2: Design Points of Design of Experiments

	A	B	C	D	E	F
1	Name	P1 - XYPlane.D4 (mm)	P2 - XYPlane.R12 (mm)	P3 - Solid Mass (kg)	P4 - Equivalent Stress Maximum (MPa)	P5 - Equivalent Elastic Strain Maximum (mm mm^-1)
2	1	28	30	0,38095	39,095	0,00019548
3	2	25,2	30	0,36571	41,681	0,00020841
4	3	30,8	30	0,39714	36,727	0,00018364
5	4	28	27	0,39316	38,145	0,00019073
6	5	28	33	0,37085	39,761	0,00019881
7	6	25,2	27	0,37893	39,619	0,0001981
8	7	30,8	27	0,40836	35,763	0,00017882
9	8	25,2	33	0,35503	41,694	0,00020847
10	9	30,8	33	0,38763	37,46	0,0001873

Figure 18. Possible design solutions

Table of Outline A12: Min-Max Search

	A	B	C	D	E	F
1	Name	P1 - XYPlane.D4 (mm)	P2 - XYPlane.R12 (mm)	P3 - Solid Mass (kg)	P4 - Equivalent Stress Maximum (MPa)	P5 - Equivalent Elastic Strain Maximum (mm mm^-1)
2	Output Parameter Minimums					
3	P3 - Solid Mass	25,2	33	**0,35503**	41,827	0,00020914
4	P4 - Equivalent Stress Maximum	30,8	27	0,40836	**35,639**	0,0001782
5	P5 - Equivalent Elastic Strain Maximum	30,8	27	0,40836	35,639	**0,0001782**
6	Output Parameter Maximums					
7	P3 - Solid Mass	30,8	27	**0,40836**	35,639	0,0001782
8	P4 - Equivalent Stress Maximum	25,2	33	0,35503	**41,827**	0,00020914
9	P5 - Equivalent Elastic Strain Maximum	25,2	33	0,35503	41,827	**0,00020914**

Figure 19. Output parameters maximum and minimum limits setup

The response surface of the output parameters as a function of the two input parameters is shown in Figures 20 to 22. The candidate point for the optimal solution is shown in Figure 23.

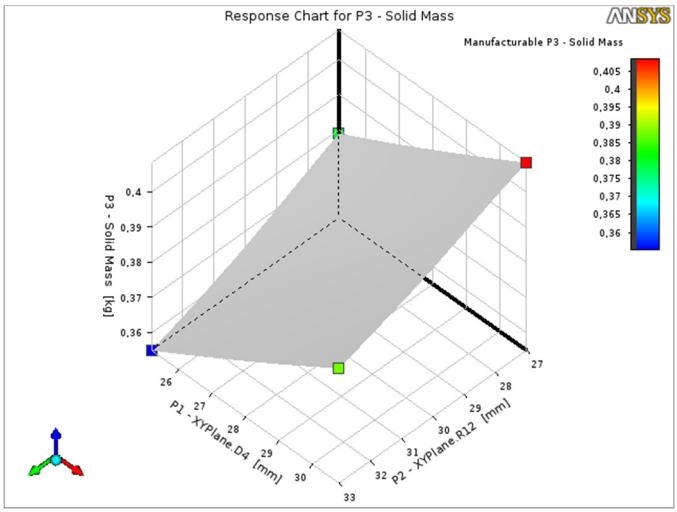

Figure 20. Response chart for P3 Solid Mass versus input parameters P1 and P2

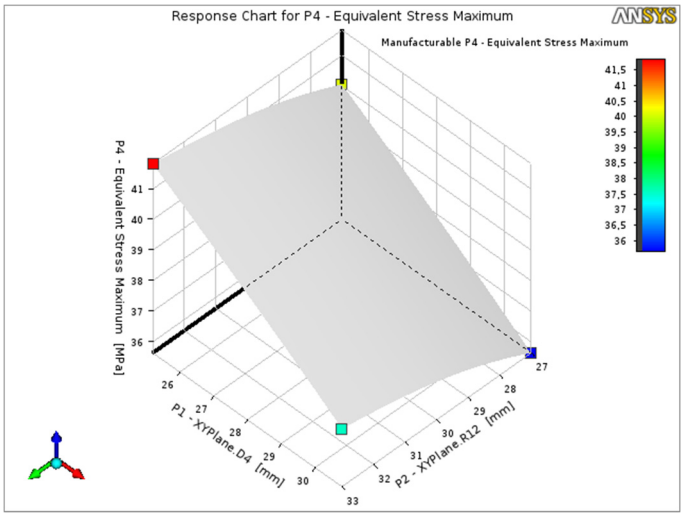

Figure 21. Response chart P4-Equivalent Stress Maximum versus input parameters P1 and P2

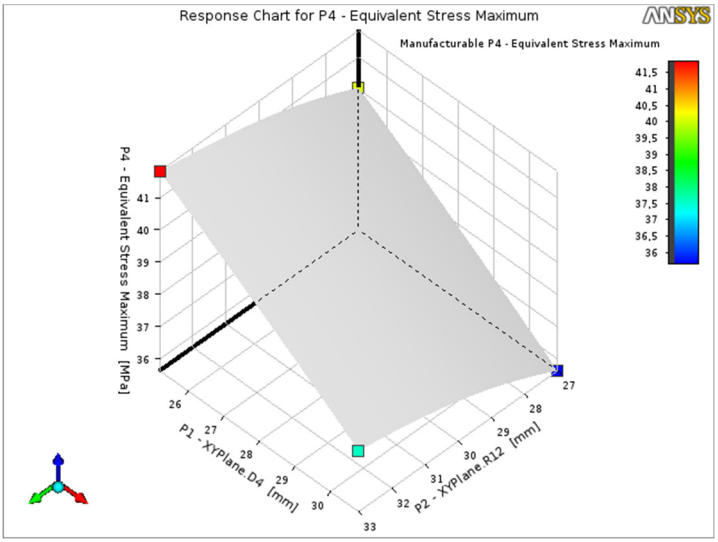

Figure 22. Response chart P5-Equivalent Elastic Strain Maximum versus input parameters P1 and P2

Table of Schematic C4: Optimization , Candidate Points

	A	B	C	D	E	F	G	H
1	Reference	Name	P1 - XYPlane.D4 (mm)	P2 - XYPlane.R12 (mm)	P3 - Solid Mass (kg)		P4 - Equivalent Stress Maximum (MPa)	P5 - Equivalent Elastic Strain Maximum (mm mm^-1)
2					Parameter Value	Variation from Reference		
3	○	Candidate Point 1	25,2	27	0,37893	-7,21 %	40,052	0,00020026
4	○	Candidate Point 1 (verified)			0,37893	-7,21 %	39,619	0,0001981
5	◉	Candidate Point 2	30,8	27	0,40836	0,00 %	35,639	0,0001782
6	○	Candidate Point 2 (verified)			0,40836	0,00 %	35,763	0,00017882
*		New Custom Candidate Point	25,2	27				

Figure 23. Optimization candidate points

4. Conclusion

This paper proposes a methodology for the dynamic study of a thermal engine connecting rod, considering its flexibility, complemented by a structural optimization algorithm with the finite element method. This methodology can be applied to any type of kinematic element in the structure of a bar mechanism.

The connecting rod of a thermal engine is a very important part, for which it is necessary to carry out a dynamic study considering its flexibility as well as structural optimization.

In conclusion, the proposed study methodology can be successfully used to be applied to other design models of connecting rods in the structure of a thermal engine, and not only.

Acknowledgment

The research was supported by the Operational Programme "Science and Education for Smart Growth", project number BG05M2OP001-2.016-0026.

References

[1] Yingkui, G., & Zhibo, Z.: Strength analysis of diesel engine crankshaft based on PRO/E and ANSYS. In 2011 Third International Conference on Measuring Technology and Mechatronics Automation. Vol. 3, pp. 362-364. IEEE. 2011.

[2] Sathish, T., Kumar, S. D., & Karthick, S.: Modelling and analysis of different connecting rod material through finite element route. Materials Today: Proceedings, 21, 971-975. 2020.

[3] Karthick, L., Michel, J., Mallireddy, N., & Vadivukarasi, L.: Modelling and analysis of an EN8 crankshaft in comparison with AISI 4130 crankshaft material. Materials Today: Proceedings. 2021.

[4] Wang, H., Yang, S., Han, L., Fan, H., & Jiang, Q.: Failure analysis of crankshaft of fracturing pump. Engineering Failure Analysis, 109, 104378. 2020.

[5] Kurbet, S. N., Kuppast, V. V., & Talikoti, B.: Material testing and evaluation of crank-shafts for structural analysis. Materials Today: Proceedings, 34, pp. 556-562. 2021.

[6] Bansal, R.: Dynamic simulation of connecting rod made of aluminum alloy using finite element analysis approach. IOSR Journal of Mechanical and Civil Engineering, 5(2), 01-05. 2013.

[7] Lu, Y., Liu, C., Zhang, Y., Wang, J., Yao, K., Du, Y., & Müller, N.: Evaluation on the tribological performance of ring/liner system under cylinder deactivation with consideration of cylinder liner deformation and oil supply. PloS one, 13(9), e0204179. 2018.